

UNCLASSIFIED

Defense Technical Information Center  
Compilation Part Notice

ADP012215

TITLE: Synthesis of Nanosized Lithium Manganate For Lithium-ion  
Secondary Batteries

DISTRIBUTION: Approved for public release, distribution unlimited

This paper is part of the following report:

TITLE: Nanophase and Nanocomposite Materials IV held in Boston,  
Massachusetts on November 26-29, 2001

To order the complete compilation report, use: ADA401575

The component part is provided here to allow users access to individually authored sections of proceedings, annals, symposia, etc. However, the component should be considered within the context of the overall compilation report and not as a stand-alone technical report.

The following component part numbers comprise the compilation report:

ADP012174 thru ADP012259

UNCLASSIFIED

## Synthesis of Nanosized Lithium Manganate For Lithium-ion Secondary Batteries

Hsien-Cheng Wang, Yueh Lin, Ming-Chang Wen, and Chung-Hsin Lu  
Department of Chemical Engineering, National Taiwan University.  
Taipei, Taiwan

### ABSTRACT

Nanosized lithium manganate powders are successfully synthesized via a newly developed reverse-microemulsion (R $\mu$ E) process. Monophasic LiMn<sub>2</sub>O<sub>4</sub> powders are obtained after calcining the precursor powders at 700°C. The particle size of the spinel compound significantly depends on the concentration of the aqueous phase. Increasing the water-to-oil volume ratio results in an increase in the particle size. While the aqueous phase is equal to 0.5 M, the size of the obtained LiMn<sub>2</sub>O<sub>4</sub> powder is around 60-70 nm. It is found that the specific capacity of nanosized LiMn<sub>2</sub>O<sub>4</sub> particles is greater than that of submicron particles. The large surface area of ultrafine particles is considered to facilitate the intercalation and deintercalation of lithium ions during the cycling test.

### INTRODUCTION

Lately, lithium-ion secondary batteries have become one of the most promising candidates in the field of rechargeable batteries owing to their high working voltage, high energy density, steady discharging properties, and long cycle life. For perfecting the performance of lithium ion batteries, the electrochemical characteristics of cathode materials have been intensively investigated. A variety of lithiated transition metal oxides including LiCoO<sub>2</sub>, LiNiO<sub>2</sub>, and LiMn<sub>2</sub>O<sub>4</sub> have been explored for utilizing as cathode electrodes in lithium-ion secondary batteries [1-4]. Among these cathode materials, lithium manganate with a spinel structure is of particular interest for using in the rechargeable cells because of its inexpensive material cost, acceptable environmental characteristics, and better safety compared to LiCoO<sub>2</sub>. However, LiMn<sub>2</sub>O<sub>4</sub> suffers the disadvantages of relatively low discharge capacity and serious capacity fading during the cycling process [6-8]. For optimizing the electrochemical performance of LiMn<sub>2</sub>O<sub>4</sub>, a great deal of efforts have been devoted to synthesize LiMn<sub>2</sub>O<sub>4</sub> powders with a controlled morphology [9,10]. A new reverse-microemulsion (R $\mu$ E) process was thus developed to control the morphology and particle size of LiMn<sub>2</sub>O<sub>4</sub> powders, developed in this study, and the electrochemical performance of the obtained powders was also evaluated.

### EXPERIMENTAL DETAILS

Lithium nitrate (LiNO<sub>3</sub>) and manganese nitrate (Mn(NO<sub>3</sub>)<sub>2</sub>) were chosen as the starting materials. The well-dispersed aqueous phase was mixed with the continuous phase that

comprised oil and surfactant. After emulsifying these starting compounds, a transparent R $\mu$ E system was successfully obtained. The R $\mu$ E system was heated and dried for preparing the precursors of the target spinel compound. The precursor powders were calcined in a tube furnace at 350°C with a heating rate of 10°C/min to obtain the LiMn<sub>2</sub>O<sub>4</sub> powders. The powders prepared at the cationic concentration of 0.5 M and 2.0 M were named as sample A and B, respectively. The crystallinity of the formed products was identified via the powder X-ray diffraction (XRD) analysis. The morphology and the particle size of the obtained powders were measured with a field emission scanning electron microscopy (FESEM). The electrochemical cell was composed of the R $\mu$ E- derived LiMn<sub>2</sub>O<sub>4</sub> powders as the cathode, lithium foil as the anode, and an electrolyte of 1 M LiPF<sub>6</sub> in ethylene carbonate (EC) and 1,2-dimethyl carbonate (DMC) solution. The charge and discharge characteristics of the cathode materials were investigated using a current density of 0.23 mA/cm<sup>2</sup> in the voltage range of 3.0 and 4.3 V.

## RESULTS AND DISCUSSION

Figure 1 illustrates the XRD patterns of the R $\mu$ E derived specimens heated at 700°C for 1 h. After analyzing the structural characteristics, these calcined powders were identified to be monophasic spinel LiMn<sub>2</sub>O<sub>4</sub> with a cubic unit cell and a space group of Fd3m. All the diffraction peaks were consistent with the data in ICDD PDF No. 35-782 [11]. It is confirmed that at the cationic concentration of 0.5 and 2.0 M, pure spinel LiMn<sub>2</sub>O<sub>4</sub> powders can be effectively synthesized using the R $\mu$ E process.

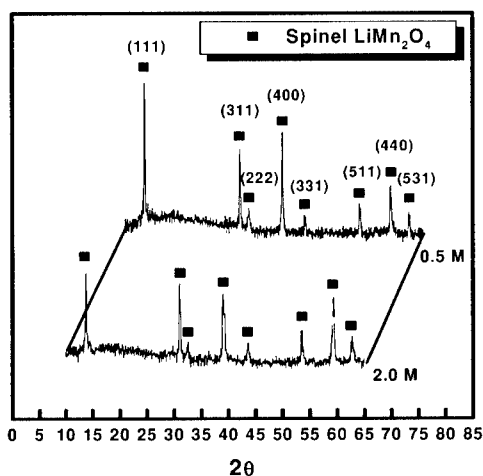


Fig. 1. XRD patterns of the R $\mu$ E-derived powders.

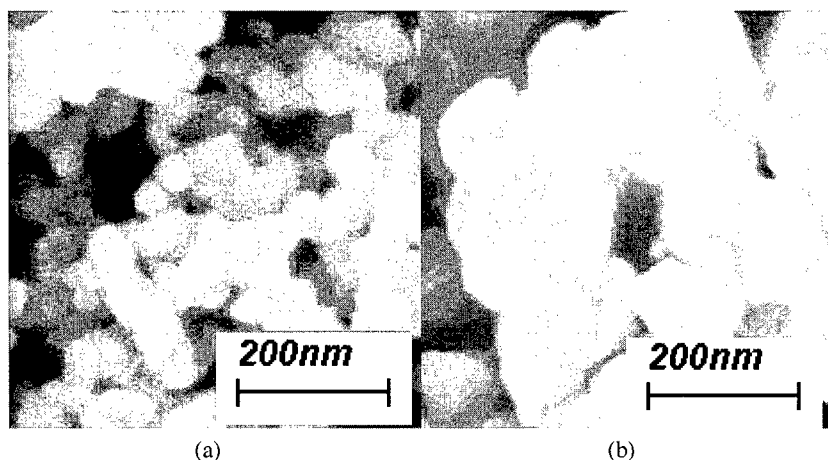


Fig. 2. The FESEM photos of the  $R_{\mu}E$ -derived powders (a) 0.5 M and (b) 2.0 M.

Figure 2 illustrates the field emission scanning electron microscopic photos of the pure spinel powders. Sample A has an uniform morphology and the particle sizes are around 60-70 nm with a narrow size distribution. Meanwhile, the mean particle size of sample B is 136 nm much larger than that of sample A. In comparison with previous solution methods, the  $R_{\mu}E$  process significantly reduces the particle size of  $LiMn_2O_4$  even down to a nanosized order. In addition, the cation concentration of the aqueous phase has a significant effect on the particle size of  $LiMn_2O_4$  powders. Increasing the cation concentration will increase the particle size of  $LiMn_2O_4$  powders. Adjusting the cation concentration is a critical issue for controlling the particle size of  $LiMn_2O_4$ .

Figure 3 shows the charge-discharge profiles for the  $700^{\circ}C$ -calcined samples cycled at  $0.23\text{ mA/cm}^2$ . The cell consisting of sample A delivered the discharge capacity of 116 mAh/g in the first cycle at room temperature. After ten cycles, the discharge capacity retained 104.2 mAh/g. For the electrochemical characteristics of the sample B, the discharge capacity in the first cycle was 92.2 mAh/g, which was smaller than that of sample A. The superior performance of sample A was attributed to the larger surface area of smaller particles, which facilitated lithium ions to participate in the intercalation/deintercalation process.

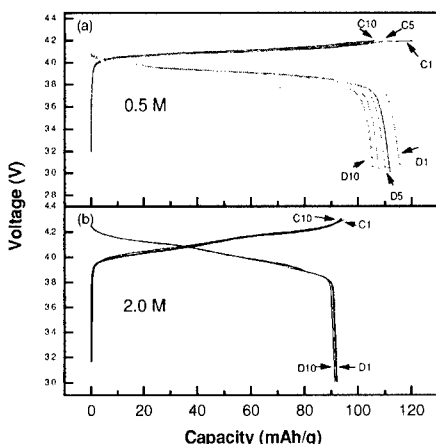


Fig. 3. Charge and discharge properties of the R $\mu$ E-derived powders cycled at the ambient temperature.

In order to investigate the cycling performance of the R $\mu$ E-derived powders at elevated temperatures, the electrochemical characteristics were also examined at 55 °C. Figure 4 illustrates the charge and discharge profiles of the 700 °C-calcined specimens. For sample A, the first-cycle discharge capacity was 98.8 mAh/g, while that of the 10th cycle was 81.0 mAh/g. As for sample B, the discharge capacities of the first and tenth cycles were 88.7 and 84.1 mAh/g, respectively. It was found that the R $\mu$ E-derived powder obtained at low cationic concentration demonstrated worse capacity fading than that derived from high cationic concentration.

The cycling stability at 55 °C and the capacity retention of the R $\mu$ E-derived powders are shown in Fig. 5. It was found that the capacity fading of sample B was less severe than that of sample A, indicating that high cationic concentration in the R $\mu$ E system is effective in suppressing the capacity fading. Figure 5(b) depicts that the capacity retention of sample A and B after 10 cycles at this temperature were 82% and 95%, respectively. It was found that the specific capacity increased with an increase in the surface area of the obtained LiMn<sub>2</sub>O<sub>4</sub> powders, however the capacity retention was completely opposite. The reason for better capacity retention of sample B at elevated temperature was its larger particle size. The enlargement of surface area facilitated the insertion and extraction of lithium ions, but also increased the dissolution of manganese ions into the electrolyte. For optimizing the electrochemical performance of the R $\mu$ E-derived LiMn<sub>2</sub>O<sub>4</sub> powders, the particles size should be precisely controlled.

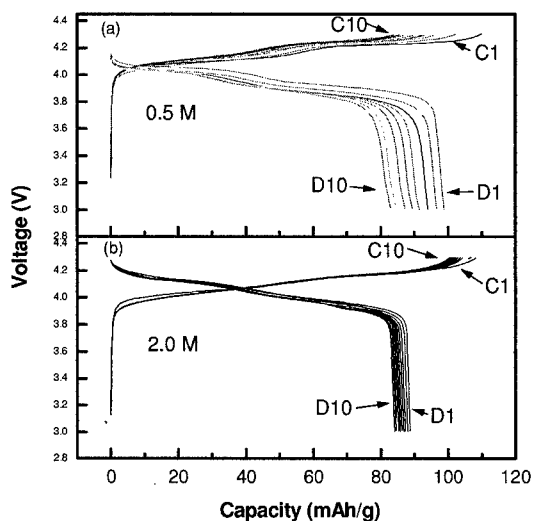


Fig. 4. Charge and discharge performance of the R $\mu$ E-derived powders at 55°C. The aqueous concentration are (a) 0.5 M and (B) 2.0 M, respectively.

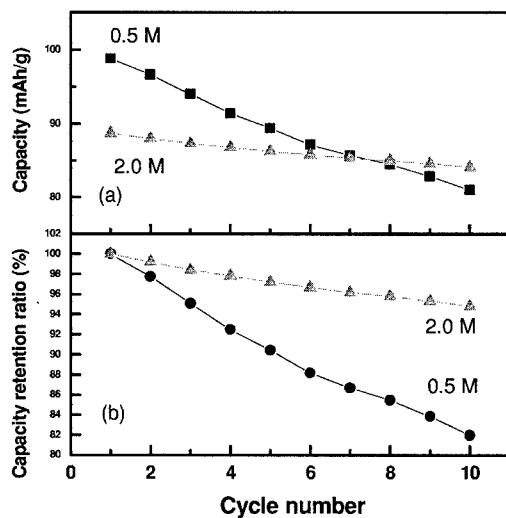


Fig. 5. Comparison of the cycling stability and the capacity retention of the R $\mu$ E-derived powders at 55°C.

## CONCLUSIONS

Monophasic nanosized  $\text{LiMn}_2\text{O}_4$  powders were successfully synthesized after calcining the precursor powders at  $700^\circ\text{C}$  for 1 h. The electrochemical performance of the obtained  $\text{LiMn}_2\text{O}_4$  powders was also examined. The particle size decreased and the surface area increased with a drop in the cationic concentration. It was found that  $\text{LiMn}_2\text{O}_4$  particles with larger surface area gave rise to a greater specific capacity but a worse cyclability at elevated temperatures. The first-cycle discharge capacities of the samples prepared from cationic concentrations of 0.5 M and 2.0 M were 98.8 and 88.7 mAh/g at  $55^\circ\text{C}$ , and the corresponding capacity retentions after ten cycles were 82% and 95%, respectively. In order to optimize the electrochemical performance of  $\text{LiMn}_2\text{O}_4$ , the control of particle size is necessary.

## REFERENCES

1. J. M. Tarascon, E. Wang, F. K. Shokoohi, W. R. McKinnon, S. Colson, *J. Electrochem. Soc.* **138**, 2859 (1991).
2. A. Momchilov, V. Manev, A. Nassalevska, *J. Power Sources* **41**, 305 (1993).
3. Z. Jiang, K. M. Abraham, *J. Electrochem. Soc.* **143**, 1591 (1996).
4. T. Ohzuku, M. Kitagawa, T. Hirai, *J. Electrochem. Soc.* **137**, 769 (1990).
5. X. H. Hu, X. P. Ai, H. X. Yang, Sh. X. Li, *J. Power Sources* **74**, 240 (1998).
6. W. Liu, G. C. Farrington, F. Chaput, B. Dunn, *J. Electrochem. Soc.* **143**, 879 (1996).
7. Y. H. Ikuhara, Y. Iwamoto, K. Kikuta, S. Hirano, *J. Mater. Res.* **14**, 3102 (1999).
8. H. J. Kweon, S. S. Kim, G. B. Kim, D. G. Park, *J. Mater. Sci. Lett.* **17**, 1697 (1998).
9. C. H. Lu, S. K. Saha, *Mater. Sci. Eng.* **B79**, 247 (2001).
10. C. H. Lu, S. W. Lin, *J. Power Sources* **93**, 14 (2001).
11. Powder Diffraction File, # 35-782. Joint Committee on Powder Diffraction Standards, Swarthmore, PA, USA.